Astronomical Notes

Astronomische Nachrichten

Founded by H. C. Schumacher in 1821

WILEY-VCH

Astron. Nachr. / AN **332**, No. 1, 51 – 56 (2011) / **DOI** 10.1002/asna.201011478

Dissipation in dynamos at low and high magnetic Prandtl numbers

A. Brandenburg⋆

NORDITA, AlbaNova University Center, Roslagstullsbacken 23, SE-10691 Stockholm, Sweden; and
Department of Astronomy, Stockholm University, SE 10691 Stockholm, Sweden

Received 2010 Oct 22, accepted 2010 Nov 18
Published online 2011 Jan 12

Key words magnetic fields – magnetohydrodynamics (MHD)

Using simulations of helically driven turbulence, it is shown that the ratio of kinetic to magnetic energy dissipation scales with the magnetic Prandtl number in power law fashion with an exponent of approximately 0.6. Over six orders of magnitude in the magnetic Prandtl number the magnetic field is found to be sustained by large-scale dynamo action of alpha-squared type. This work extends a similar finding for small magnetic Prandtl numbers to the regime of large magnetic Prandtl numbers. At large magnetic Prandtl numbers, most of the energy is dissipated viscously, lowering thus the amount of magnetic energy dissipation, which means that simulations can be performed at magnetic Reynolds numbers that are large compared to the usual limits imposed by a given resolution. This is analogous to an earlier finding that at small magnetic Prandtl numbers, most of the energy is dissipated resistively, lowering the amount of kinetic energy dissipation, so simulations can then be performed at much larger fluid Reynolds numbers than otherwise. The decrease in magnetic energy dissipation at large magnetic Prandtl numbers is discussed in the context of underluminous accretion found in some quasars.

1 Introduction

The magnetic fields in astrophysical bodies often have a pronounced large-scale component that is associated with large-scale dynamo action. Examples are the cyclic magnetic fields in late-type stars such as the Sun and the magnetic spirals in many galaxies, including even irregular galaxies; see Beck et al. (1996) for a review. In addition, all observed magnetic fields also have a significant small-scale component that may either be the result of turbulent motions distorting the large-scale field, or, alternatively, it could be the result of what is known as small-scale dynamo action (Cattaneo 1999).

Much of our knowledge about large-scale and small-scale dynamos has come from numerical simulations; see Brandenburg & Subramanian (2005) for a review. It is clear that, in order for simulations to approach an astrophysically interesting regime, one wants to make both the magnetic diffusivity and the kinematic viscosity as small as possible. This means that the magnetic and fluid Reynolds numbers should be as large as possible for a given numerical resolution, N^3. The relevant criterion for sufficient numerical resolution is that the kinetic and magnetic energy spectra should develop an exponentially decaying dissipative subrange at a wavenumber that is at least a factor of 10 below the Nyquist frequency, $k_{\rm Ny}=\pi N/L$. In practice, for example, with a simulation at a resolution of 512^3 mesh points, one can hardly exceed values of the magnetic and fluid Reynolds number of about 500–700 (e.g. Brandenburg 2009). However, as will be discussed in more detail in this paper, this empirical constraint on the resolution really only applies if the ratio of magnetic and fluid Reynolds numbers is about unity. This ratio is also referred to as the magnetic Prandtl number, $\mathrm{Pr_M}$, and there is hardly any system where this number is unity. In galaxies and galaxy clusters this number tends to be very large, while in stars and stellar accretion discs it is quite small. Also liquid metals used in laboratory experiments have small $\mathrm{Pr_M}$. Therefore, much of what has been learnt from numerical simulations at $\mathrm{Pr_M}\approx1$ has to be re-examined in cases of low and high values of $\mathrm{Pr_M}$.

The purpose of this paper is to focus on the relative importance of viscous and ohmic dissipation rates at different values of $\mathrm{Pr_M}$. Often, viscous and ohmic dissipation are only treated "numerically" by making sure the code is stable. In such cases, viscosity and magnetic diffusivity are usually not even stated explicitly in the equations, suggesting that these terms are negligible and not important. This is of course not the case, as can be illustrated by considering the case of quasars that belong to the most luminous objects in the sky. The discovery of the first quasar, 3C 273, is nicely explained by Rhodes (1978) in a popular magazine. Indeed, 3C 273, has about 2×10^{12} times the luminosity of the Sun and is indeed the brightest one in the sky. This quasar would not shine at all if it was not for the effect of microphysical viscosity that leads to viscous dissipation. But how important is viscous dissipation compared with ohmic dissipation? In order to address this problem we need to understand the effects of both viscosity and mag-

⋆ Corresponding author: brandenb@nordita.org

netic diffusivity in a turbulent system where the magnetic field is self-sustained by dynamo action. In this paper we review briefly some recent work on dynamos in the regime of small $\mathrm{Pr_M}$ and turn then to the investigation of large $\mathrm{Pr_M}$.

2 Small magnetic Prandtl number dynamos

In the last 6 years the issue of low magnetic Prandtl numbers, $\mathrm{Pr_M}=\nu/\eta$, has become a frequently discussed topic in the dynamo community. This is the regime where the magnetic diffusivity η is large compared with the kinematic viscosity ν. Already over a decade ago, Rogachevskii & Kleeorin (1997) noticed that for small-scale dynamos the critical value of the magnetic Reynolds number, $\mathrm{Re_M}$, for the onset of dynamo action should rise from a value around 35 at $\mathrm{Pr_M}=1$ to values around 400 for small values of $\mathrm{Pr_M}$. Here, $\mathrm{Re_M}=u_{\rm rms}/\eta k_{\rm f}$ is defined with respect to the wavenumber $k_{\rm f}$ of the energy-carrying eddies and the rms velocity, $u_{\rm rms}$. However, the result of Rogachevskii & Kleeorin was not widely recognized at the time. In 2004, simulation began to address this point systematically. Simulations of Schekochihin et al. (2004) and Haugen et al. (2004) provided clear indications that $\mathrm{Re_M^{crit}}$ rises, and the results of Schekochihin et al. (2005) might have even suggested that the critical value of $\mathrm{Re_M}$ for small-scale dynamo action might have become infinite for $\mathrm{Pr_M}\approx0.1$.

Meanwhile, Boldyrev & Cattaneo (2004) provided an attractive framework for understanding this behavior. Given that the energy spectrum of the small-scale dynamo peaks at the resistive scale, which is the smallest possible scale at which the motions can still overcome resistive damping, one must ask what are the properties of the flow at this scale.

In the original scenario of Kazantsev (1968), the small-scale dynamo works through a velocity field that is random, but essentially laminar and of large scale. In a simulation this can be realized by choosing a large magnetic Prandtl number, so the magnetic Reynolds number is much larger than the fluid Reynolds number. However, subsequent studies show that small-scale dynamo action can also occur for $\mathrm{Pr_M}$ of order unity. Both for $\mathrm{Pr_M}=1$ and for $\mathrm{Pr_M}\gg1$ one finds that the spectral magnetic energy increases with wavenumber proportional to $k^{3/2}$.

A qualitatively new feature emerges when $\mathrm{Pr_M}$ is small. In that case the wavenumber corresponding to the resistive scale decreases and lies in the inertial range of the turbulence. This property is crucial because in the inertial range the velocity field is "rough", i.e. over a spatial interval δx the velocity difference $\delta u=u(x+\delta x)-u(x)$ scales like $\delta u\sim\delta x^{\zeta}$ where $\zeta<1$. Thus, the finite difference quotient of the velocity, $\delta u/\delta x$, diverges with decreasing δx, provided δx is still bigger than the viscous cutoff scale. According to Boldyrev & Cattaneo (2004), the critical magnetic Reynolds number increases with increasing roughness.

In all situations that have been simulated, the wavenumber range of the spectra has been too limited so that they are affected by cutoff effects both at large and small scales. In particular, only in simulations beyond 1024^3 meshpoints the spectra are shallower than $k^{-5/3}$. This is referred to as the bottleneck effect and is believed to be a physical effect (Falkovich 1994; Dobler et al. 2003; Frisch et al. 2008). One reason, however, why it is not usually seen in wind tunnel or atmospheric boundary layer turbulence is the fact that one measures in these cases only one-dimensional spectra. In order to obtain three-dimensional spectra, one has to differentiate those data, i.e. (Dobler et al. 2003)

$$E_{\rm 3D}=-{\rm d}E_{\rm 1D}/{\rm d}\ln k\,. \tag{1}$$

Accepting thus the physical reality of the bottleneck effect, it becomes plausible that the critical magnetic Reynolds number for the onset of small-scale dynamo action reaches a maximum around $\mathrm{Pr_M}=0.1$, and that it decreases somewhat for smaller values of $\mathrm{Pr_M}$. This is indeed what the simulations of Iskakov et al. (2007) suggest.

Let us now switch to large-scale dynamos. Their excitation conditions are characterized by the dynamo number which, for helical turbulence and in the absence of shear, is just

$$C_\alpha=\frac{\alpha}{\eta_{\rm T}k_1}\approx\epsilon_{\rm f}\iota\frac{k_{\rm f}}{k_1}. \tag{2}$$

Here, $k_1=2\pi/L$ is the minimal wavenumber in the domain of size L and we have inserted standard approximations for the α effect, $\alpha=\frac{1}{3}\tau\overline{\boldsymbol{w}\cdot\boldsymbol{u}}$, and the turbulent magnetic diffusivity, $\eta_{\rm t}=\frac{1}{3}\tau\overline{\boldsymbol{u}^2}$. Here, $\boldsymbol{u}=\boldsymbol{U}-\overline{\boldsymbol{U}}$ is the fluctuating velocity, i.e. the difference between the actual velocity $\boldsymbol{U}$ and the mean velocity $\overline{\boldsymbol{U}}$, $\tau\approx(u_{\rm rms}k_{\rm f})^{-1}$ is the turnover time, $\boldsymbol{w}=\boldsymbol{\nabla}\times\boldsymbol{u}$ is the fluctuating vorticity, $\epsilon_{\rm f}=\overline{\boldsymbol{w}\cdot\boldsymbol{u}}/k_{\rm f}\overline{\boldsymbol{u}^2}$ is a measure for the relative helicity, and $\iota=1+3/\mathrm{Re_M}$ is a correction factor of order unity for sufficiently large values of $\mathrm{Re_M}$. It turns out that in all cases the spectra of magnetic energy are at the largest scale approximately independent of $\mathrm{Re_M}$ for $\mathrm{Pr_M}$ between 1 and 10^{-3}. This was shown in Brandenburg (2009) and will here be extended to $10\leq\mathrm{Pr_M}\leq10^3$.

At larger wavenumbers there is a striking difference in the magnetic energy spectra between $\mathrm{Pr_M}=1$ and $\ll1$ in that the resistive cutoff wavenumber moves toward smaller values. At the same time, the kinetic energy spectrum becomes progressively steeper, leaving less kinetic energy to dissipate. This has two important consequences. First of all, the fractional kinetic energy dissipation decreases with decreasing $\mathrm{Pr_M}$ proportional to $\mathrm{Pr_M^{1/2}}$ (Brandenburg 2009). On the other hand, the decrease of $\epsilon_{\rm K}$ implies that the demand for numerical resolution becomes less stringent. This, in turn, means that one can increase the value of Re beyond the normally established empirical limits. An important goal of the present paper is the demonstration that the same is also true in the opposite limit of $\mathrm{Pr_M}\gg1$.

3 The model

Our model is similar to that presented in Brandenburg (2001, 2009), where we solve the hydromagnetic equations

Table 1 Summary of import input and output parameters for the runs reported in this paper.

$\mathrm{Pr_M}$	Re	$\mathrm{Re_M}$	$\tilde{\epsilon}_\mathrm{K}$	$\tilde{\epsilon}_\mathrm{M}$	k_K	k_M	Res.
10^{-3}	4400	4	0.01	0.99	426	8	512^3
10^{-2}	2325	23	0.04	0.96	344	25	512^3
10^{-1}	1175	118	0.13	0.87	286	81	512^3
10^{0}	455	455	0.39	0.61	179	201	512^3
10^{1}	20	200	0.76	0.24	24	99	256^3
10^{2}	9	850	0.90	0.10	14	263	256^3
10^{3}	0	425	0.99	0.01	3	129	256^3
10^{3}	1	1175	0.99	0.01	5	234	256^3

for velocity $\boldsymbol{U}$, logarithmic density $\ln\rho$, and magnetic vector potential $\boldsymbol{A}$ for an isothermal gas in the presence of an externally imposed helical forcing function $\boldsymbol{f}$,

$$\frac{\partial \boldsymbol{U}}{\partial t} = -\boldsymbol{U}\cdot\boldsymbol{\nabla}\boldsymbol{U} - c_\mathrm{s}^2\boldsymbol{\nabla}\ln\rho + \boldsymbol{f} + (\boldsymbol{J}\times\boldsymbol{B} + \boldsymbol{\nabla}\cdot 2\rho\nu\mathsf{S})/\rho, \quad (3)$$

$$\frac{\partial \ln\rho}{\partial t} = -\boldsymbol{U}\cdot\boldsymbol{\nabla}\ln\rho - \boldsymbol{\nabla}\cdot\boldsymbol{U}, \quad (4)$$

$$\frac{\partial \boldsymbol{A}}{\partial t} = \boldsymbol{U}\times\boldsymbol{B} - \mu_0\eta\boldsymbol{J}. \quad (5)$$

Here, $\boldsymbol{B} = \boldsymbol{\nabla}\times\boldsymbol{A}$ is the magnetic field, $\boldsymbol{J} = \boldsymbol{\nabla}\times\boldsymbol{B}/\mu_0$ is the current density, μ_0 is the vacuum permeability, c_s is the isothermal speed of sound, and $\mathsf{S}_{ij} = \frac{1}{2}(U_{i,j} + U_{j,i}) - \frac{1}{3}\delta_{ij}\boldsymbol{\nabla}\cdot\boldsymbol{U}$ is the traceless rate of strain tensor. We consider a triply periodic domain of size L^3, so the smallest wavenumber in the domain is $k_1 = 2\pi/L$. The forcing function consists of eigenfunctions of the curl operator with positive eigenvalues and is therefore fully helical with $\boldsymbol{f}\cdot\boldsymbol{\nabla}\times\boldsymbol{f} = k\boldsymbol{f}^2$, where $3.5 \le k/k_1 \le 4.5$ is the chosen wavenumber interval of the forcing function, whose average value is referred to as $k_\mathrm{f} \approx 4\,k_1$. The amplitude of $\boldsymbol{f}$ is such that the Mach number is $u_\mathrm{rms}/c_\mathrm{s} \approx 0.1$, so compressive effects are negligible (Dobler et al. 2003). As in Brandenburg (2009), we choose as initial conditions a Beltrami field of low amplitude. The initial velocity is zero and the initial density is uniform with $\rho = \rho_0 = \mathrm{const}$, so the volume-averaged density remains constant, i.e., $\langle\rho\rangle = \rho_0$.

In our simulations we change the values of magnetic and fluid Reynolds numbers,

$$\mathrm{Re_M} = u_\mathrm{rms}/\eta k_\mathrm{f}, \quad \mathrm{Re} = u_\mathrm{rms}/\nu k_\mathrm{f}, \quad (6)$$

such that the ratio $\mathrm{Re_M}/\mathrm{Re} = \mathrm{Pr_M}$ has the desired value between 10^{-3} and 10^3, and we monitor the resulting kinetic and magnetic energy dissipation rates per unit volume,

$$\epsilon_\mathrm{K} = \langle 2\nu\rho\mathsf{S}^2\rangle, \quad \epsilon_\mathrm{M} = \langle\eta\mu_0\boldsymbol{J}^2\rangle, \quad (7)$$

whose sum, $\epsilon_\mathrm{T} = \epsilon_\mathrm{K} + \epsilon_\mathrm{M}$, will be used to define the fractional dissipation rates, $\tilde{\epsilon}_\mathrm{K} = \epsilon_\mathrm{K}/\epsilon_\mathrm{T}$ and $\tilde{\epsilon}_\mathrm{M} = \epsilon_\mathrm{M}/\epsilon_\mathrm{T}$. We use the fully compressible PENCIL CODE [1] for all our calculations. We recall that, for the periodic boundary conditions under consideration, $\langle 2\mathsf{S}^2\rangle = \langle\boldsymbol{W}^2\rangle + \frac{4}{3}\langle(\boldsymbol{\nabla}\cdot\boldsymbol{U})^2\rangle$, highlighting thus the analogy between $\boldsymbol{W} = \boldsymbol{\nabla}\times\boldsymbol{U}$ and $\boldsymbol{J}$ in the incompressible case.

[1] http://www.pencil-code.googlecode.com

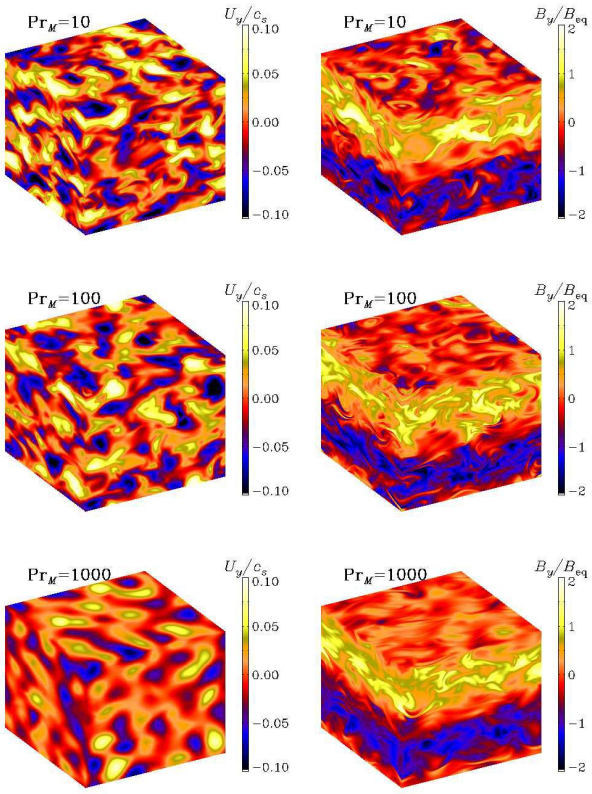

Fig. 1 (online colour at: www.an-journal.org) Visualization of U_y and B_y on the periphery of the computational domain for $\mathrm{Pr_M}$ ranging from 10 to 1000 at a resolution of 256^3 mesh points.

4 Results

In Table 1 we summarize the parameters of runs with $\mathrm{Pr_M}$ between 10^{-3} and 10^3. The runs with $10^{-3} \le \mathrm{Pr_M} \le 1$ are those presented already in Brandenburg (2009) using 512^3 mesh points, while those with $10 \le \mathrm{Pr_M} \le 1000$ are new ones and have been performed using 256^3 mesh points. In all cases, either Re or $\mathrm{Re_M}$ were close to the maximum possible limit at a given resolution. Indeed, for $\mathrm{Pr_M} = 10^{-3}$ we were able to reach $\mathrm{Re} = 4400$ (for 512^3 mesh points) while for $\mathrm{Pr_M} = 10^3$ we could go to $\mathrm{Re_M} = 1200$ (for 256^3 mesh points).

We note that in all cases the total energy dissipation is approximately the same. This is perhaps not so surprising, because we keep the amplitude of the forcing function the same. However, the constancy of the energy dissipation rate implies that the rate of energy injection must also be always the same and thus independent of $\mathrm{Pr_M}$. This means that the flow properties of the eddies at the energy-carrying scale must be essentially independent of $\mathrm{Pr_M}$.

In Fig. 1 we present visualizations of the y component of velocity and magnetic field at the periphery of the computational domain for the new results with $\mathrm{Pr_M} \ge 10$ and in Fig. 2 we show spectra of kinetic and magnetic energies, $E(k)$ and $M(k)$, respectively, for all values of $\mathrm{Pr_M}$

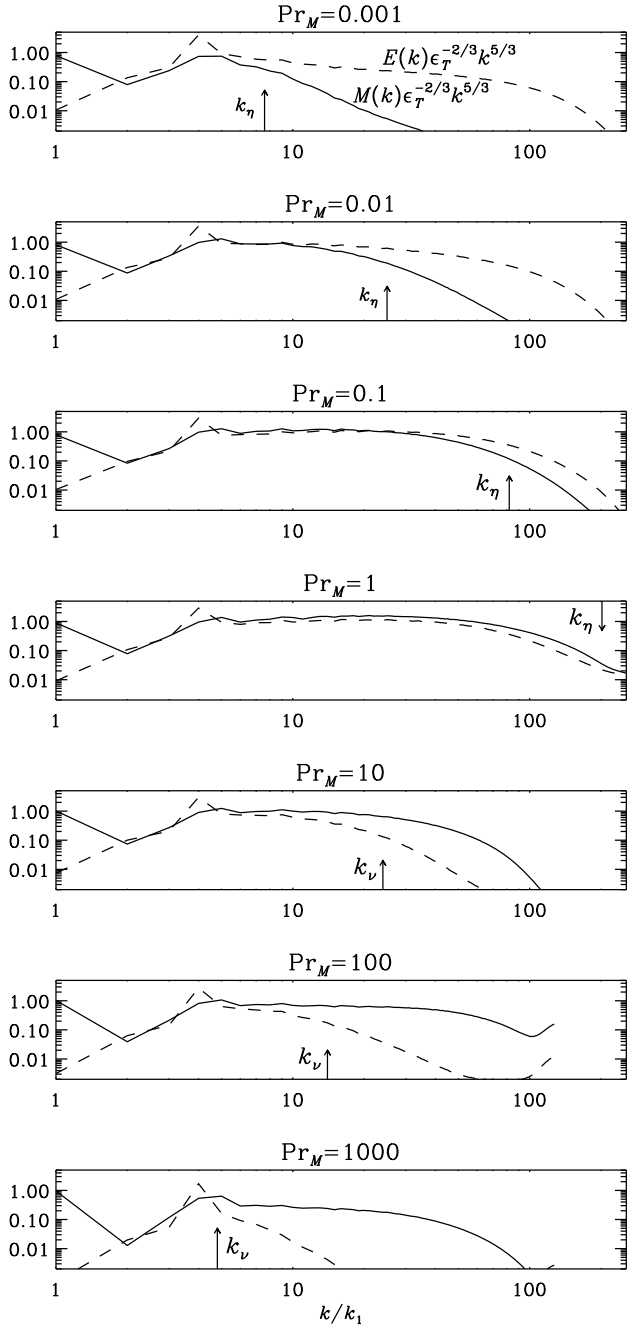

Fig. 2 Compensated kinetic and magnetic energy spectra in the saturated regime for $\mathrm{Pr_M}=10^{-3}$ to 10^3. The spectra are compensated by $\epsilon_{\mathrm{T}}^{-2/3}k^{5/3}$, where ϵ_{T} is the sum of kinetic and magnetic energy dissipation rates. The ohmic dissipation wavenumber, $k_\eta=(\epsilon_{\mathrm{M}}/\eta^3)^{1/4}$, is indicated by an arrow.

between 10^{-3} and 10^3. In the velocity pattern one can clearly make out the typical scale of the dominant eddies, whose wave length is about 1/4 of the size of the box. The magnetic field also shows a turbulent component, but there is a much stronger large-scale component superposed. This is essentially the Beltrami field which is of the form $\overline{\boldsymbol{B}}=(\cos k_1 z,\,\sin k_1 z,\,0)$, although its wavevector could have pointed in any of the other two coordinate directions, $(0,\,\cos k_1 x,\,\sin k_1 x)$ and $(\sin k_1 y,\,0,\,\cos k_1 y)$ would have been equally probably alternatives. We recall that all these fields are indeed the eigenfunctions of an α^2 dynamo problem (e.g., Brandenburg & Subramanian 2005), and they also emerge as the dominant field in helically driven turbulence. It is clear that in a triply periodic domain such as that considered here, these fields require a resistive time to reach full saturation. For all further details we refer to Brandenburg (2001), where such a system was studied in full detail.

Next, we consider the spectra of kinetic and magnetic energies in Fig. 2 which are normalized such that $\int E(k)\,\mathrm{d}k=\frac{1}{2}\langle\rho\boldsymbol{U}^2\rangle$ and $\int M(k)\,\mathrm{d}k=\frac{1}{2}\langle\boldsymbol{B}^2/\mu_0\rangle$. It is evident from the spectra that with increasing values of $\mathrm{Pr_M}$, the viscous dissipation wavenumber, $k_\nu=(\epsilon_{\mathrm{K}}/\nu^3)^{1/4}$, moves to smaller and smaller values. Analogously to the case of $\mathrm{Pr_M}\ll 1$, this implies that most of the injected energy gets dissipated by the shorter of the two cascades – leaving only a reduced amount of energy for the other cascade. This means that the corresponding diffusion coefficient can be decreased further, without creating numerical difficulties.

It appears that it is not only the energy input at the small wavenumber end of the relevant cascade that is decreased, but that there is possibly a continuous removal of energy along the cascade, making the spectral index slightly steeper than $-5/3$. For example, for $\mathrm{Pr_M}=10^{-3}$ the spectral slope of $E(k)$ is about -2.2, while for $\mathrm{Pr_M}=10^3$ the spectral slope of $M(k)$ is about -2.0.

It is quite extraordinary that in all these cases the nature of the large-scale dynamo is virtually unchanged, even though $\mathrm{Pr_M}$ is varied by 6 orders of magnitude. The reason is that in all cases the dynamo number, C_α, exceeds the critical value for dynamo action, $C_\alpha^{\mathrm{crit}}=1$. Looking at Eq. (2), we see that C_α is dominated by the scale separation ratio, which is here $k_{\mathrm{f}}/k_1\approx 4$. Furthermore, because the turbulence is nearly fully helical, we have $\epsilon_{\mathrm{f}}\approx 1$, and since $\mathrm{Re_M}\gg 1$, we have $\iota\approx 1$. Thus, we have $C_\alpha>1$ for all runs. We recall also that the saturation amplitude of the field is essential given by the square root of the scale separation ratio (Brandenburg 2001), which is about 2 in units of the equipartition field strength. This is in reasonable agreement with the simulation results; see Fig. 2, where we show the resulting spectra for all the runs.

Next, we plot in Fig. 3 the ratio of kinetic to magnetic energy dissipation rates. In agreement with Brandenburg (2009), we find that the ratio is approximately proportional to $\mathrm{Pr_M^{1/2}}$, although a better fit is now provided by $\epsilon_{\mathrm{K}}/\epsilon_{\mathrm{M}}\approx 0.6\,\mathrm{Pr_M^{0.6}}$. The reason for such a scaling is unclear. However, from Eq. (7) one can see that in the ratio $\epsilon_{\mathrm{K}}/\epsilon_{\mathrm{M}}$ there is an implicit proportionality with respect to $\mathrm{Pr_M}$. Assuming, for simplicity, $\langle 2\mathsf{S}^2\rangle\approx\langle\boldsymbol{W}^2\rangle\approx W_{\mathrm{rms}}^2$, we see that

$$\frac{\epsilon_{\mathrm{K}}}{\epsilon_{\mathrm{M}}}\approx\rho\frac{\nu}{\eta}\frac{W_{\mathrm{rms}}^2}{J_{\mathrm{rms}}^2}\propto\mathrm{Pr_M^n},\qquad(8)$$

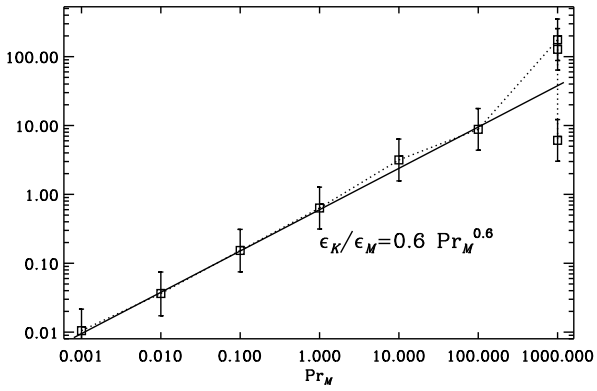

Fig. 3 Dependence of the ratio of the dissipation rates on $\mathrm{Pr_M}$.

so

$$\frac{W_{\rm rms}}{J_{\rm rms}} \propto \mathrm{Pr_M}^{(n-1)/2} \approx \mathrm{Pr_M}^{-1/4} \ldots \mathrm{Pr_M}^{-1/6}, \quad (9)$$

where we have assumed that n lies between 1/2 and 2/3, which bracket the results seen here and in Brandenburg (2009). These scalings are surprising in view of the usually expected individual scalings, namely $W_{\rm rms} \propto \nu^{-1/2}$ and $J_{\rm rms} \propto \eta^{-1/2}$ (cf. Brandenburg & Subramanian 2005).

In order to illuminate the issue further, we ask whether not only the ratio $\epsilon_{\rm K}/\epsilon_{\rm M}$ scales with $\mathrm{Pr_M}$, but whether $\epsilon_{\rm K}$ and $\epsilon_{\rm M}$ are individually proportional to Re and $\mathrm{Re_M}$, respectively. In Fig. 4 we plot $\epsilon_{\rm K}$ versus Re (blue, solid symbols) and $\epsilon_{\rm M}$ versus $\mathrm{Re_M}$ (red, open symbols). The scatter is now much larger than in Fig. 3, and it seems that the scaling exponent might even be as large as $n = 2/3$.

We mentioned earlier that the total dissipation rate, $\epsilon_{\rm T}$, is nearly independent of $\mathrm{Pr_M}$. However, this is only true when we look the the dimensional value of $\epsilon_{\rm T}$. It is customary to consider the normalized dissipation rate,

$$C_\epsilon = \frac{\epsilon_{\rm T}}{u_{\rm 1D}^3/L}, \quad (10)$$

where $u_{\rm 1D} = u_{\rm rms}/\sqrt{3}$ is the one-dimensional rms velocity and $L = 3\pi/4k_{\rm f}$ is conventionally used as the integral scale (Pearson et al. 2004). In the second and third panels of Fig. 4 we compare C_ϵ with $C_{\epsilon 0}$, which is based on the maximum value of $u_{\rm 1D}$ in all the runs. The difference is caused by the fact that $u_{\rm rms}$ drops to rather low values in the large-$\mathrm{Pr_M}$ regime. Part of this goes into magnetic energy, but it is not enough to make up for this difference.

It is important to realize that, on average, $\epsilon_{\rm M}$ is just the same as the rate of work done against the Lorentz force, $-\langle \boldsymbol{U}\cdot(\boldsymbol{J}\times\boldsymbol{B})\rangle$. This becomes evident when considering the flow of energy in our system:

$$\langle \rho \boldsymbol{U}\cdot\boldsymbol{f}\rangle \rightarrow \begin{cases} & \rightarrow \langle 2\rho\nu \mathsf{S}^2\rangle \\ -\langle \boldsymbol{U}\cdot(\boldsymbol{J}\times\boldsymbol{B})\rangle & \rightarrow \langle \eta\mu_0 \boldsymbol{J}^2\rangle. \end{cases} \quad (11)$$

Here, $\langle \rho \boldsymbol{U}\cdot\boldsymbol{f}\rangle \approx \epsilon_{\rm T}$ is the rate of energy injection into the system by the forcing term. Normally, in the hydrodynamic case, $\langle 2\rho\nu\mathsf{S}^2\rangle$, or $\langle \nu \boldsymbol{W}^2\rangle$ in the incompressible case, stay

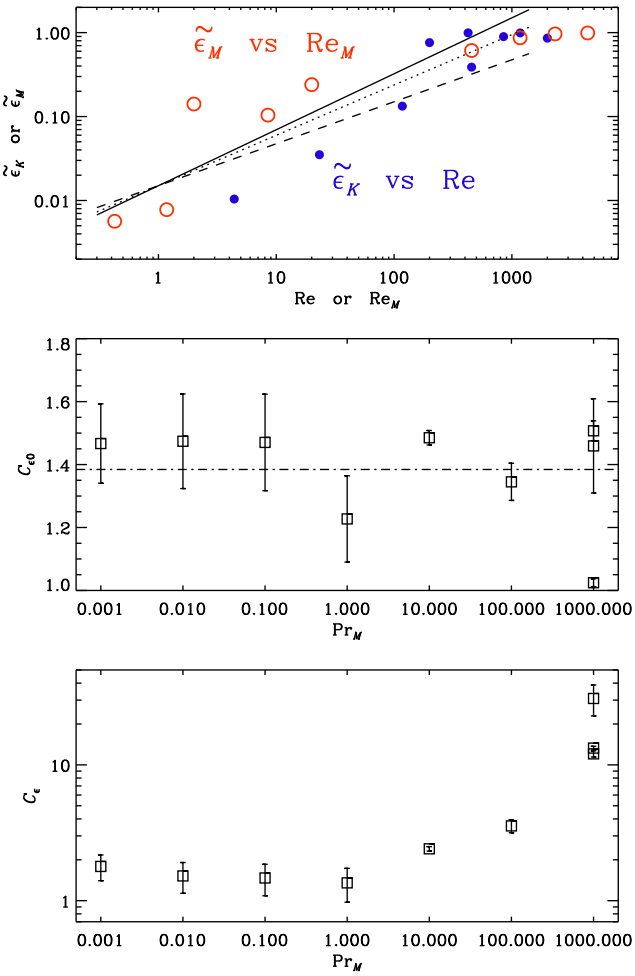

Fig. 4 (online colour at: www.an-journal.org) *Top*: dependence of $\epsilon_{\rm K}$ on Re (blue, solid symbols) and $\epsilon_{\rm M}$ on $\mathrm{Re_M}$ (red, open symbols). The solid line has the slope 2/3, while the dotted and dashed lines have slopes 0.6 and 0.5, respectively. *Middle and bottom*: scalings of $C_{\epsilon 0}$ and C_ϵ versus $\mathrm{Pr_M}$.

constant as ν is decreased. In the case with dynamo action, however, a decrease in ν allows the dynamo to tap more energy, so $-\langle \boldsymbol{U}\cdot(\boldsymbol{J}\times\boldsymbol{B})\rangle$ and $\epsilon_{\rm M}$ increase at the expense of $\epsilon_{\rm K}$. This is indicated by the fact $\epsilon_{\rm K}/\epsilon_{\rm M}$ is found to be proportional to $(\nu/\eta)^n$, so $\epsilon_{\rm K}$ decreases as ν decreases. This decease is weak in the sense that $n \approx 1/2 \ldots 2/3$ is less than unity, but it is certainly no longer independent of ν as it would be in the purely hydrodynamic case.

In view of the application to quasars, i.e. accretion discs in active galactic nuclei, it is relevant to consider the fraction of energy that goes into the heating of electrons. Indeed, such discs are known to be underluminous, which led to the standard paradigm of advection-dominated accretion (Narayan & Yi 1994; Abramowicz et al. 1995). Alternatively, this might be associated with the small value of the ratio $\epsilon_{\rm M}/\epsilon_{\rm T}$, for which we find

$$\frac{\epsilon_{\rm M}}{\epsilon_{\rm T}} = \frac{\epsilon_{\rm M}}{\epsilon_{\rm M}+\epsilon_{\rm K}} \propto \frac{1}{1+\mathrm{Pr_M^n}}. \quad (12)$$

Using standard accretion disc theory, Balbus & Henri (2008) find that $\mathrm{Pr_M}$ depends on the distance R from the black hole and is proportional to $R^{-9/8}$. In particular, they find that $\mathrm{Pr_M}$ exceeds unity within about 50 Schwarzschild radii. This would dramatically decrease ϵ_M in the inner parts and might be sufficient to explain underluminous accretion. However, this proposal hinges on several assumptions: (i) that the viscous heating heats the ions and not the electrons, (ii) that the resistive dissipation energizes electrons rather than ions, (iii) that the discs are essentially collisionless and, finally, (iv) that the magnetohydrodynamic approximation is then still applicable.

5 Conclusions

The present work has shown that the ratio of kinetic to magnetic energy dissipation follows one and the same relationship with $\mathrm{Pr_M}$ both for small and large values. An important additional condition obeyed by all our runs is, however, that the magnetic Reynolds number is large enough for dynamo action to occur. This constitutes an important difference between our current results for large-scale dynamos and those mentioned in the first section for small-scale dynamos. An important consequence of such scaling is the fact that at extreme values of the magnetic Prandtl number, larger Reynolds numbers can be tolerated by the numerical scheme at a resolution that would be insufficient if the magnetic Prandtl number were unity. This was shown previously for $\mathrm{Pr_M}=10^{-3}$, in which case fluid Reynolds numbers of 4500 were possible at a resolution of 512^3 meshpoints, while for $\mathrm{Pr_M}=1$ it was only possible to reach Reynolds numbers of less that 700. Both cases obeyed the empirical constraint that the spectral *kinetic* energy has developed a clear dissipative subrange with an exponential decay shortly before the Nyquist frequency. In the opposite case of large $\mathrm{Pr_M}$, here $\mathrm{Pr_M}=10^3$, it was possible to reach magnetic Reynolds numbers of 1000 at 256^3 mesh points. In this case the *magnetic* energy spectrum has developed a dissipative subrange shortly before the Nyquist frequency, although it was less convincing for $\mathrm{Pr_M}=10^2$.

The reason for the value of the exponent n in the power law relation between the energy dissipation ratio $\epsilon_\mathrm{K}/\epsilon_\mathrm{M}$ and $\mathrm{Pr_M}$ remains unclear. At this point we cannot be certain that it is $n=0.6$ and not, for example, 1/2 or 2/3. One source of error might come from the fact that at extreme values of $\mathrm{Pr_M}$ the effects of numerical viscosity associated with the advection operator are no longer negligible. For the third-order time step used in the PENCIL CODE, the numerical viscosity operator takes the form $-\nu_2^\mathrm{CFL}\nabla^4$ where $\nu_2^\mathrm{CFL}=u_\mathrm{rms}\delta x^3 C_\mathrm{CFL}^3/24$ is a numerical hyperviscosity[2] that depends on the mesh size δx and the Courant-Friedrich-Levy number C_CFL, whose default value is 0.4, but the code would still be numerically stable for $C_\mathrm{CFL}=0.9$. If such numerical effects do begin to play a role, we must expect that the effective values of $\mathrm{Pr_M}$ are less extreme, which means that the n would have been underestimated and that n might be 2/3 or even larger.

While earlier work focussed on the dependence of ϵ_M on $\mathrm{Pr_M}$ (Blackman & Field 2008), no clear conclusion about the dissipation ratio $\epsilon_\mathrm{K}/\epsilon_\mathrm{M}$ seems to have emerged. For example, if ϵ_K and ϵ_M were independent of viscosity and magnetic diffusivity, the ratio $\epsilon_\mathrm{K}/\epsilon_\mathrm{M}$ would have been constant. Instead, we find that ϵ_K decreases when Re decreases, and likewise, ϵ_M decreases when $\mathrm{Re_M}$ decreases. On the other hand, one must be cautious when applying results regarding the dependence on $\mathrm{Re_M/Re}$ $(=\mathrm{Pr_M})$ for large values of Re and $\mathrm{Re_M}$, because we may still not be in an asymptotic parameter regime. It is therefore important to extend this work to larger values of Re and $\mathrm{Re_M}$ and to go to larger numerical resolution.

Acknowledgements. I thank the referee for making several useful suggestions. The computations have been carried out on the National Supercomputer Centre in Linköping and the Center for Parallel Computers at the Royal Institute of Technology in Sweden. This work was supported in part by the Swedish Research Council, grant 621-2007-4064, and the European Research Council under the AstroDyn Research Project 227952.

References

Abramowicz, M.A., Chen, X., Kato, S., Lasota, J.-P., Regev, O.: 1995, ApJ 438, L37
Balbus, S.A., Henri, P.: 2008, ApJ 674, 408
Beck, R., Brandenburg, A., Moss, D., Shukurov, A., Sokoloff, D.: 1996, ARA&A 34, 155
Blackman, E.G., Field, G.B.: 2008, MNRAS 386, 1481
Boldyrev, S., Cattaneo, F.: 2004, Phys. Rev. Lett. 92, 144501
Brandenburg, A.: 2001, ApJ 550, 824
Brandenburg, A.: 2009, ApJ 697, 1206
Brandenburg, A., Subramanian, K.: 2005, Phys. Rev. 417, 1
Cattaneo, F.: 1999, ApJ 515, L39
Dobler, W., Haugen, N.E.L., Yousef, T.A., Brandenburg, A.: 2003, Phys. Rev. E 68, 026304
Falkovich, G.: 1994, Phys. Fluids 6, 1411
Frisch, U., Kurien, S., Pandit, R., Pauls, W., Ray, S.S., Wirth, A., Zhu, J.-Z.: 2008, Phys. Rev. Lett. 101, 144501
Haugen, N.E.L., Brandenburg, A., Dobler, W.: 2004, Phys. Rev. E 70, 016308
Iskakov, A.B., Schekochihin, A.A., Cowley, S.C., McWilliams, J.C., Proctor, M.R.E.: 2007, Phys. Rev. Lett. 98, 208501
Kazantsev, A.P.: 1968, Sov. Phys. JETP 26, 1031
Narayan, R., Yi, I.: 1994, ApJ 428, 13
Pearson, B.R., Yousef, T.A., Haugen, N.E.L., Brandenburg, A., Krogstad, P. Å.: 2004, Phys. Rev. E 70, 056301
Rhodes, R.: 1978, Playboy 25, 140
Rogachevskii, I., Kleeorin, N.: 1997, Phys. Rev. E 56, 417
Schekochihin, A.A., Cowley, S.C., Maron, J.L., McWilliams, J.C.: 2004, Phys. Rev. Lett. 92, 054502
Schekochihin, A.A., Haugen, N.E.L., Brandenburg, A., Cowley, S.C., Maron, J.L., McWilliams, J.C.: 2005, ApJ 625, L115

[2] See page 118 of the PENCIL CODE manual, http://www.nordita.org/software/pencil-code/doc/manual.pdf.

